ALGORITHM FOR COMPUTATION OF THE ACOUSTIC PLANE-WAVE REFLECTION COEFFICIENT OF THE OCEAN BOTTOM

by

DAVID RICHARD MARTINEZ

B.S., New Mexico State University
(1976)

SUBMITTED IN PARTIAL FULFILLMENT OF THE
REQUIREMENTS FOR THE DEGREE OF

ELECTRICAL ENGINEER

at the

WOODS HOLE OCEANOGRAPHIC INSTITUTION

and at the

MASSACHUSETTS INSTITUTE OF TECHNOLOGY

and

MASTER OF SCIENCE IN ELECTRICAL ENGINEERING

at the

MASSACHUSETTS INSTITUTE OF TECHNOLOGY

June 1979

Signature of Author .....
Joint Program in Oceanographic Engineering, Woods Hole Oceanographic Institution - Massachusetts Institute of Technology, and the Department of Electrical Engineering, Massachusetts Institute of Technology, May, 1979

Certified by.... .....
Thesis Supervisor

Certified by.... .....
Thesis Supervisor

Accepted by.... .....
Chairman, Joint Committee for Oceanographic Engineering, Woods Hole Oceanographic Institution - Massachusetts Institute of Technology

ALGORITHM FOR COMPUTATION OF THE ACOUSTIC PLANE-WAVE REFLECTION COEFFICIENT OF THE OCEAN BOTTOM

by

DAVID RICHARD MARTINEZ

Submitted to the Department of Electrical Engineering on May 11, 1979, in partial fulfillment of the requirements for the degrees of Master of Science and Electrical Engineer.

ABSTRACT

For a spherical acoustic wave incident on a horizontally stratified ocean bottom, the reflected pressure field and the plane-wave reflection coefficient are related through a two-dimensional spatial-wavenumber Fourier transform. An algorithm is proposed to evaluate the plane-wave reflection coefficient from the bottom reflected field as a function of angle of incidence.

The algorithm is based on the "Projection-Slice" theorem associated with the two-dimensional Fourier transform. This technique is implemented to evaluate the plane-wave reflection coefficient for a perfectly reflecting ocean bottom and for an isovelocity-low speed ocean bottom model.

Thesis Supervisor: Alan V. Oppenheim
Title: Professor of Electrical Engineering

Thesis Supervisor: George V. Frisk
Title: Assistant Scientist, W.H.O.I.

ACKNOWLEDGEMENT

I am thankful to Dr. Robert Porter for suggesting the problem as a possible thesis topic during the early stages of the research.

My supervisors, Prof. Al Oppenheim and Dr. George Frisk, were more than invaluable at every phase of the project. They both taught me to appreciate the rewards of constant dedication to research. Their guidance, advice, and understanding are gratefully acknowledged.

I wish to thank Dr. Earl Hays for providing valuable criticism and support which were essential to the completion of the thesis.

I am thankful to Miss Susan Smith for her excellence in typing the draft and final manuscript.

Finally, special thanks to Miss Denice Wye for her patience, constant encouragement, and stimulation that were needed to devote myself to long hours of continuous work.

TABLE OF CONTENTS

TABLE OF CONTENTS (cont.)

TABLE OF FIGURES

Page No.

Page No.

Page No.

CHAPTER 1

INTRODUCTION

For a horizontally stratified ocean bottom, the plane-wave reflection coefficient as a function of incident angle and frequency contains all the information necessary for the solution of acoustic problems in the ocean. It is needed, for example, in implementing ray tracing programs and in evaluating the performance of bottomed and suspended hydrophones. Hence, it is of interest to implement an algorithm to numerically calculate it from experimental bottom-reflected data.

For many years, the measurement of the plane-wave reflection coefficient from bottom-reflected data has been an important area of research. The plane-wave reflection coefficient is a complex function and it has been difficult to measure its magnitude and phase as a function of horizontal wavenumber and frequency. Some of the early techniques, in an attempt to measure the magnitude, were based on approximating the bottom-reflected signal by the field from an image source multiplied by the reflection coefficient at the specular angle of incidence. This approximation, which is based on the geometrical acoustic approximation, assumed high values of acoustic frequency with source and receivers many wavelengths from the bottom and no significant influence of interface waves on the result[16]. Based on this approximation, Liebermann[9] (1948) conducted an experiment at a constant high frequency (24 kHz) to measure the magnitude of the reflection coefficient from the

resultant of the interference between the direct and reflected waves. Another application of the geometrical acoustics approximation was implemented by Hastrup[8] (1970) to measure the magnitude as a function of frequency by forming a ratio between the Fourier transforms of the bottom-reflected and direct signals.

In an effort to compute a more accurate estimate of the plane-wave reflection coefficient, other techniques were developed based on the exact Hankel transform relationship between the plane-wave reflection coefficient and the bottom-reflected field, the assumptions being a horizontally stratified ocean bottom where all acoustic properties were only a function of depth, and an acoustic point source. Based on this relationship, DiNapoli[3] (1977) calculated the magnitude by approximating the exact Hankel transform to be of the Fourier type integral, assuming the source to be located many wavelengths in-range from the hydrophone. This method provided close results for some region of the specular angle domain, with poor convergence for normal and grazing angles of incidence. Similarly, Schoenberg[15] (1978) started with the exact Hankel transform, and formed a linear combination of the reflected data points. This technique was based on the Backus-Gilbert inversion method. An estimate of the magnitude and phase was then computed by minimizing a norm under the least-squares criterion. This general procedure had the advantage that it

included signals with additive noise, and the disadvantage of large amounts of implementation time.

This thesis presents a different approach to measuring the magnitude and phase of the plane-wave reflection coefficient as a function of horizontal wavenumber and frequency. The proposed algorithm is based on interpreting the exact relationship between the bottom-reflected field and the plane-wave reflection coefficient in the form of a zero-order Hankel transform, making it suitable to the application of a recent method by Oppenheim, Frisk, and Martinez[10] to compute an n^{th}-order Hankel transform. The technique is based on the "Projection-Slice" theorem associated with the two-dimensional Fourier transform. The result of this approach permits the estimation of the effect of a horizontally stratified ocean bottom on all propagating compressional waves in the water, including plane waves at real angles of incidence and inhomogeneous plane waves propagating parallel to the ocean floor and decaying exponentially in the vertical direction away from the bottom.

The details of the algorithm are presented in Chapter 2. The chapter introduces a derivation of the exact Hankel transform between the plane-wave reflection coefficient and the bottom-reflected field, with the discrete processing to determine the reflection coefficient from samples of the reflected data. In Chapters 3 and 4, the algorithm is examined in two simple ocean bottom models. Chapter 3 considers a perfectly reflecting ocean

bottom for which the reflected field is known analytically. Chapter 4 studies the estimation of the reflection coefficient for an isovelocity-low speed bottom.

As a generalization of the algorithm, some of the most common Hankel transforms are presented in Appendix I and are compared to their exact theoretical answers. The Fortran program is included.

CHAPTER 2

PLANE-WAVE REFLECTION COEFFICIENT AND ITS COMPUTATION

2.1 Introduction

The ocean and its environment are very complex and difficult to analyze when trying to infer some of the ocean bottom properties. It is possible to simplify the complexity by including physical assumptions and still preserve a model of experimental interest. The following sections introduce the model, its fundamentals, and the details of the algorithm in computing the plane-wave reflection coefficient from the bottom-reflected data.

2.2 Ocean Model and Assumptions

In finding a general model that represents the ocean and its environment, the sound velocity, density, and attenuation must be included, since they are primarily the properties that dictate the behavior of propagation of sound in the ocean. The first assumption, to simplify the complexity of the model, is that the sound velocity and density are of constant magnitude over the water column and that in the ocean bottom they are only a function of depth, i.e., a horizontally stratified ocean bottom. Also, the attenuation is assumed to be zero in the water column and a function of frequency and depth in the bottom. In Figure 2.1, the general model is shown, including the source-receiver geometry.

In order to simplify the model even further, a distinction

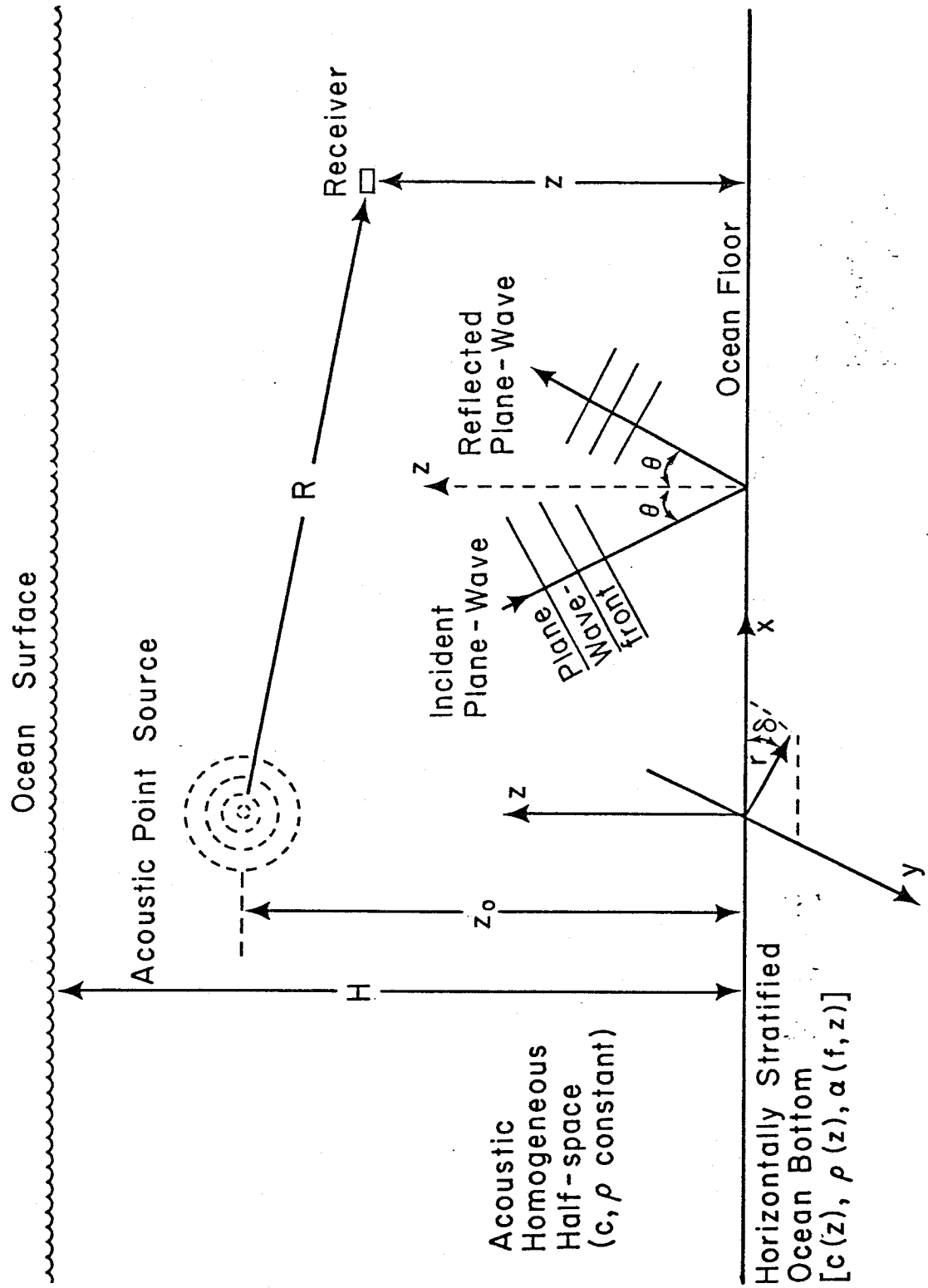

Figure 2.1. General ocean model.

must be made between a model for propagation of sound in shallow water and deep water. Shallow water propagation is considered when the acoustic source wavelength is of the order of the water depth. If the source wavelength is of much smaller magnitude than the water depth, the process is modeled as deep water propagation; that is,

$$\lambda = \frac{c}{f} \simeq H \qquad \text{shallow water}$$

$$\lambda = \frac{c}{f} << H \qquad \text{deep water}$$

where λ = wavelength

c = sound velocity in the water

f = acoustic source frequency

H = water depth

If the frequency of interest is on the order of 200 Hz or more, corresponding to a wavelength less than 7 m, the example falls in the category of deep water propagation when performing the experiment in locations of water depth greater than a hundred meters. The model can then be simplified by considering the water column as a half-space, when the source and receivers are a small number of wavelengths away from the bottom. This implies that any surface-relfected energy can be neglected, since it is

sufficiently time-separated from the direct and bottom-reflected signals.

This general simplified model, shown in Figure 2.1, permits an analytic derivation of the wave equation

$$\nabla^2 p(x,y,z,t) = \frac{1}{c^2} \frac{\partial^2 p(x,y,z,t)}{\partial t^2} \qquad (2.2.1)$$

where $p(x,y,z,t)$ = acoustic pressure

x,y,z = rectangular coordinates (see Figure 2.1)

and leads to an expression which represents the acoustic field for propagating waves in the ocean. The derivation of Eq. 2.2.1 can be found in reference (5).

In what follows, we present a solution to this wave equation to find an analytic relationship between the plane-wave reflection coefficient and the reflected pressure field.

Solution to the Wave Equation

In spherical coordinates (see Figure 2.1), Eq. 2.2.1 has the following form

$$\frac{\partial^2 p}{\partial R^2} + \frac{2}{R} \frac{\partial p}{\partial R} = \frac{1}{c^2} \frac{\partial^2 p}{\partial t^2} \qquad (2.2.2)$$

where $R^2 = x^2 + y^2 + (z-z_0)^2$

z = receiver height

z_0 = source height

A general solution to this equation is

$$p(R,t) = \frac{1}{R}\left[f_1(R-ct) + f_2(R+ct)\right] \qquad (2.2.3)$$

where $f_1(R-ct)$ = spherical waves radiating away from the source

$f_2(R+ct)$ = spherical waves radiating towards the source

$\frac{1}{R}$ = spherical spreading loss

The physical constraint that no energy radiates from infinity towards the source makes

$$f_2(R+ct) = 0$$

thus

$$p(R,t) = \frac{1}{R} f_1(R-ct) \qquad (2.2.4)$$

A simple source in acoustics can be assumed to a pulsating sphere of small radius with harmonic time dependence. It radiates spherical waves, and when its radius is small compared to the wavelength it is referred to as point source. Then, the acoustic pressure has the form

$$p(R,t) = s\,\frac{e^{j(K_1 R - wt)}}{R} \qquad (2.2.5)$$

where $K_1 = w/c$ = angular frequency/sound velocity; and it satisfies the wave equation since it is of the same form as Eq. 2.2.4. Equivalently,

$$p(R,t) = s\,P(R,w)e^{-jwt} \qquad (2.2.6)$$

where s = acoustic source strength

$P(R,w)$ = range dependent response

e^{-jwt} = harmonic time dependence

If, instead of a point source with harmonic time dependence, a more general source is used, the pressure field is found by evaluating a Fourier transform over angular frequency w of the product between the range dependent response of the medium and the angular frequency response of this general source.

In the derivation that follows, omission of the time dependence e^{-jwt} is made, and a point source of constant angular frequency w and of strength $s = 1$ is assumed in Eq. 2.2.6. Thus,

$$P(R) = \frac{e^{jK_1 R}}{R} \qquad (2.2.7)$$

where K_1 = natural wavenumber = w/c

$w = 2\pi f$

f = acoustic source frequency

c = sound velocity

$$R^2 = x^2 + y^2 + (z-z_0)^2 = r^2 + (z-z_0)^2$$

Reflection Coefficient $\leftrightarrow$ Pressure Field Relationship

The study of spherical waves is often simplified by representing them in terms of plane waves[1]. In Eq. 2.2.7, we see that the spherical wave representing the pressure field satisfies constant phase at any point at the same radial distance from the source. This corresponds to wavefronts of spherical shape. On the other hand, plane waves hold constant phase at any point on a plane perpendicular to the direction of propagation. Upon encountering a boundary where there exists a change in sound speed and/or density, a plane wave can be interpreted in terms of a ray incident at an angle θ (see Figure 2.1). The spatial rate of propagation of this plane wave in the (x,y) plane is defined as the horizontal wavenumber and it corresponds to

$$K = K_1 \sin \theta \qquad (2.2.8)$$

where K = horizontal wavenumber

K_1 = natural wavenumber = w/c

θ = angle of incidence

The plane-wave reflection coefficient modulates each of the plane waves incident at different angles or, equivalently, at each horizontal wavenumber. If we model the horizontally stratified ocean bottom as composed of a number of discrete layers, the plane-wave reflection coefficient can be analytically calculated for simple types of ocean bottoms by satisfying the boundary conditions of continuity of normal stress and displacement at the water-bottom interface. A more detailed discussion of some analytically computed reflection coefficients is considered in Chapters 3 and 4.

An interpretation of spherical waves in terms of plane waves is achieved by forming a superposition of cylindrical functions constrained to satisfy the cylindrical wave equation[5]. That is,

$$P(r,z) = \frac{e^{jK_1 R}}{R} = \int_0^\infty F(K) J_0(Kr) e^{j\sqrt{K_1^2 - K^2}\,|z-z_0|} dK \qquad (2.2.9)$$

where $J_0(Kr)$ = zero-order Bessel function

$|z-z_0|$ = vertical distance traveled by propagating waves from source to receiver

$F(K)$ = a function of horizontal wavenumber (K) to satisfy the equality

and, from Eq. 2.2.6,

$$p(r,z,t) = s\, P(r,z)\, e^{-jwt} \qquad (2.2.10)$$

If this equation is substituted in the cylindrical wave equation,

$$\frac{\partial^2 p(r,z,t)}{\partial r^2} + \frac{1}{r}\frac{\partial p(r,z,t)}{\partial r} + \frac{\partial^2 p(r,z,t)}{\partial z^2} = \frac{1}{c^2}\frac{\partial^2 p(r,z,t)}{\partial t^2} \qquad (2.2.11)$$

the result is

$$\frac{d^2 J_0(Kr)}{dr^2} + \frac{1}{r}\frac{dJ_0(Kr)}{dr} + K^2 J_0(Kr) = 0 \qquad (2.2.12)$$

which is indeed satisfied[17].

F(K) can be calculated by interpreting Eq. 2.2.9 as an inverse Hankel transform type integral[14]. Thus, at $z = z_0$,

$$\frac{F(K)}{K} = \int_0^\infty e^{jK_1 r} J_0(Kr)\,dr \qquad (2.2.13)$$

which corresponds to a Hankel transform, and it can be analytically calculated by assuming K_1 to have a small positive imaginary part[17], i.e., the medium is slightly absorbing. The result is

$$F(K) = j\frac{K}{\sqrt{K_1^2 - K^2}} \qquad (2.2.14)$$

Substituting Eq. 2.2.14 into Eq. 2.2.9,

$$\frac{e^{jK_1 R}}{R} = j\int_0^\infty \frac{e^{j\sqrt{K_1^2 - K^2}\,|z-z_0|}}{\sqrt{K_1^2 - K^2}} J_0(Kr)\,K\,dK \qquad (2.2.15)$$

which constitutes the interpretation of a spherical wave in terms of plane waves. The integrand, in the (x,y,z) coordinate system, corresponds to plane waves, as will be illustrated more explicitly in Chapter 3. The left-hand side of the equation is the unreflected field from a point source located in a homogeneous medium.

The reflected field can be similarly interpreted by recalling that the plane-wave reflection coefficient modulates each of the plane waves upon reflection from a boundary. If we assume a horizontally stratified ocean bottom, the plane-wave reflection coefficient would only be a function of horizontal wavenumber when constant frequency is assumed[6]. The reflected pressure field is then

$$P_R(r,z,z_0) = j \int_0^{\infty} R(K) \frac{e^{j\sqrt{K_1^2-K^2}\,(z+z_0)}}{\sqrt{K_1^2-K^2}} J_0(Kr)\, K\, dK \qquad (2.2.16)$$

where $P_R(r,z,z_0)$ = bottom-reflected field

$R(K)$ = plane-wave reflection coefficient

$z+z_0$ = total vertical distance traveled by a reflected propagating plane wave

It is of interest to know R(K) since it contains information that characterizes the assumed horizontally stratified ocean bottom. In the following section, the details of the algorithm to compute R(K) from the bottom-reflected field $P_R(r,z,z_0)$ are presented.

2.3 Evaluation of the Plane-Wave Reflection Coefficient

In the previous section, we indicated that the bottom-reflected field can be interpreted in terms of plane waves modulated by the plane-wave reflection coefficient R(K); that is,

$$P_R(r,z,z_0) = j \int_0^\infty R(K) \frac{e^{j\sqrt{K_1^2-K^2}\,(z+z_0)}}{\sqrt{K_1^2-K^2}} J_0(Kr)\, K\, dK \qquad (2.3.1)$$

This equation can be reduced to be of the form of a Hankel transform by redefining the integrand. Define,

$$G(K,z,z_0) = j\, R(K) \frac{e^{j\sqrt{K_1^2-K^2}\,(z+z_0)}}{\sqrt{K_1^2-K^2}} \qquad (2.3.2)$$

as the reflection process Green's function, then Eq. 2.3.1 reduces to

$$P_R(r,z,z_0) = \int_0^\infty G(K,z,z_0)\, J_0(Kr)\, K\, dK \qquad (2.3.3)$$

If we assume the source and receivers to be at a constant height from the bottom, z and z_0 become constant parameters, and Eq. 2.3.3 simplifies to

$$P_R(r) = \int_0^\infty G(K)\, J_0(Kr)\, K\, dK \qquad (2.3.4)$$

Eq. 2.3.4 constitutes a zero-order inverse Hankel transform. The

plane-wave reflection coefficient R(K) can be represented in terms of the bottom-reflected field $P_R(r)$ by computing the Hankel transform. Thus,

$$G(K) = \int_0^\infty P_R(r)\ J_0(Kr)\ rdr \qquad (2.3.5)$$

This transformation can be proved valid by substituting Eq. 2.3.5 in Eq. 2.3.4 and factoring the result using the orthogonality property of Bessel functions[17]

$$\int_0^\infty J_0(Kr)\ J_0(\hat{K}r)\ rdr = \frac{\delta(\hat{K}-K)}{\sqrt{\hat{K}K}} \qquad (2.3.6)$$

where $$\delta(\hat{K}-K) = \begin{cases} 1; & \hat{K} = K \\ 0; & \hat{K} \neq K \end{cases}$$

Substituting Eq. 2.3.2 in Eq. 2.3.5, the relationship between the plane-wave reflection coefficient and the bottom-reflected field is

$$R(K) = -jK_z\ e^{-jK_z(z+z_0)} \int_0^\infty P_R(r)\ J_0(Kr)\ rdr \qquad (2.3.7)$$

where K_z = vertical wavenumber = $\sqrt{K_1^2 - K^2}$

The plane-wave reflection coefficient R(K) identifies a very

general class of ocean bottom. The only constraint is that the ocean bottom be horizontally stratified.

In computing R(K), the method exploits the circular symmetry of the bottom-reflected field $P_R(r)$ in the (x,y) plane ($r^2 = x^2 + y^2$). It is this property that allows a Hankel transform to be equivalently defined in the form of a two-dimensional Fourier transform.

From Figure 2.1,

$$\begin{aligned} x &= r \cos \delta \\ y &= r \sin \delta \end{aligned} \tag{2.3.8}$$

Similarly, R(K) is also circularly symmetric in the (K_x, K_y) plane. Thus,

$$\begin{aligned} K_x &= K \cos \alpha \\ K_y &= K \sin \alpha \\ R(K) &= R(\sqrt{K_x^2 + K_y^2}) \end{aligned} \tag{2.3.9}$$

An integral representation of $J_0(Kr)$ is[17]

$$J_0(Kr) = \frac{1}{2\pi} \int_0^{2\pi} e^{-jKr \cos (\alpha - \delta)} d\delta \tag{2.3.10}$$

valid for any angle α.

Substituting Eq. 2.3.10 in Eq. 2.3.7,

$$R(K) = -jK_z\, e^{-jK_z (z+z_0)}\, \frac{1}{2\pi} \int_0^{\infty} P_R(r)\, r \int_0^{2\pi} e^{-jKr \cos(\alpha-\delta)}\, d\delta\, dr \tag{2.3.11}$$

and with a change of variables, Eq. 2.3.11 becomes

$$R(K_x,K_y) = -jK_z\, e^{-jK_z(z+z_0)}\, \frac{1}{2\pi} \iint_{-\infty}^{\infty} P_R(x,y)\, e^{-jK_x x}\, e^{-jK_y y}\, dx\, dy \tag{2.3.12}$$

which, from Eq. 2.3.5, implies

$$G(K_x,K_y) = \frac{1}{2\pi} \iint_{-\infty}^{\infty} P_R(x,y)\, e^{-jK_x x}\, e^{-jK_y y}\, dx\, dy \tag{2.3.13}$$

The integral in Eq. 2.3.12 constitutes a two-dimensional Fourier transform. Since the Fourier transform of a circularly symmetric function is also circularly symmetric, $P_R(x,y)$ and $R(K_x,K_y)$ are completely specified by their corresponding radial slices. The technique in evaluating Eq. 2.3.12 is an application of a recent method by Oppenheim, Frisk, and Martinez[10] based on the "projection-slice" theorem. In essence, this theorem states that a slice at any angle through a two-dimensional trans-

form is the one-dimensional transform of a projection at the same angle of the original two-dimensional function. In the case of a circularly symmetric function R(K), the one-dimensional Fourier transform of a projection of $P_R(x,y)$ specifies the entire two-dimensional Fourier transform $R(K_x,K_y)$. Therefore, Eq. 2.3.12 can be equivalently specified by

$$R(K_x) = -jK_z\, e^{-jK_z(z+z_0)}\, \frac{1}{2\pi} \int_{-\infty}^{\infty} P_y(x)\, e^{-jK_x x}\, dx \qquad (2.3.14)$$

where $K_z = \sqrt{K_1^2 - K_x^2}$

and

$$P_y(x) = 2 \int_0^{\infty} P_R\left(\sqrt{x^2+y^2}\right)\, dy \qquad (2.3.15)$$

is the projection of the circularly symmetric function $P_R\left(\sqrt{x^2+y^2}\right)$ onto the x-axis.

The sampling theorem[2] states that a band-limited function, with zero spectral content for $K \geq K_{max}$, is completely specified by the values of its samples located at a distance Δx apart provided $\Delta x \leq \pi/K_{max}$. That is, if $P_R(r)$ is a band-limited function, i.e., $G(K) = 0$ for $K \geq K_{max}$, then Eqs. 2.3.14 and 2.3.15 can be computed by evaluating a one-dimensional discrete Fourier transform and a simple summation, respectively. This can be shown by first interpreting Eqs. 2.3.14 and 2.3.15 as follows:

$$R(K_x) = -jK_z\, e^{-jK_z(z+z_0)}\, \frac{\Delta x}{2\pi} \sum_{n=-\infty}^{\infty} P_y(n\Delta x)\, e^{-jK_x n\Delta x} \qquad (2.3.16)$$

and

$$P_y(n\Delta x) = 2\Delta y \sum_{\ell=0}^{\infty} P_R\left(\sqrt{(n\Delta x)^2+(\ell\Delta y)^2}\right) \qquad (2.3.17)$$

provided only that $\Delta x \leq \frac{\pi}{K_{max}}$ and $\Delta y \leq \frac{2\pi}{K_{max}}$.

The plane-wave reflection coefficient in Eq. 2.3.16 can then be efficiently calculated at N equally spaced values $\Delta K = \frac{1}{N}\frac{2\pi}{\Delta x}$, using the one-dimensional FFT. Thus,

$$R(m\Delta K) = -jK_m\, e^{-jK_m(z+z_0)}\, \frac{\Delta x}{2\pi} \sum_{i=-\infty}^{\infty} \sum_{n=0}^{N-1} P_y(\Delta x(n+iN))\, e^{-jnm\Delta x\Delta K} \qquad (2.3.18)$$

or

$$R(m\Delta K) = -jK_m\, e^{-jK_m(z+z_0)}\, \frac{\Delta x}{2\pi} \sum_{n=0}^{N-1} \left[\sum_{i=-\infty}^{\infty} P_y(\Delta x(n+iN))\right] e^{-j\frac{2\pi}{N}nm} \qquad (2.3.19)$$

where $K_m = \sqrt{K_1^2-(m\Delta K)^2}$

If the samples $P_y(x)$ constitute a finite-length sequence of length $\leq N\Delta x$, the evaluation of the plane-wave reflection coefficient reduces to

$$R(m\Delta K) = -jK_m\, e^{-jK_m(z+z_0)}\, \frac{\Delta x}{2\pi} \sum_{n=0}^{N-1} P_y(n\Delta x)\, e^{-j\frac{2\pi}{N}nm} \qquad (2.3.20)$$

and

$$P_y(n\Delta x) = 2\Delta y \sum_{\ell=0}^{\infty} P_R\left(\sqrt{(n\Delta x)^2+(\ell\Delta y)^2}\right) \qquad (2.3.21)$$

2.4 Circular Windows

The computation of the plane-wave reflection coefficient R(K) from samples of the bottom-reflected field has reduced to a one-dimensional FFT and a summation. That is,

$$R(m\Delta K) = -jK_m\, e^{-jK_m(z+z_0)}\, \frac{\Delta x}{2\pi} \sum_{n=0}^{N-1} P_y(n\Delta x)\, e^{-j\frac{2\pi}{N}nm} \qquad (2.4.1)$$

and

$$P_y(n\Delta x) = 2\Delta y \sum_{\ell=0}^{\infty} P_R\left(\sqrt{(n\Delta x)^2+(\ell\Delta y)^2}\right) \qquad (2.4.2)$$

where $\Delta x \leq \frac{\pi}{K_{max}}$; $\Delta y \leq \frac{2\pi}{K_{max}}$

$$\Delta K = \frac{1}{N}\frac{2\pi}{\Delta x}$$

$$K_m = \sqrt{K_1^2 - (m\Delta K)^2}$$

These equations are strictly satisfied when $P_R(r)$ is a band-limited function, or equivalently $G(K) = 0$ for $K \geq K_{max}$. However, in actual physical systems, a function is not band-limited in the strict sense. In most cases, on the other hand, there is some range of wavenumber outside of which the wavenumber spectrum is of sufficiently small magnitude to be assumed zero with negligible error.

Another point of importance in the evaluation of Eq. 2.4.1 is the assumption that the projection $P_y(n\Delta x)$ is a finite-length sequence of length $\leq N\Delta x$, which allows Eq. 2.3.16 to reduce to the form of Eq. 2.4.1. However, a function with most of the energy confined to a finite bandwidth in the wavenumber domain, in the range or x-domain, is often of considerable magnitude for an appreciable distance. This forces the algorithm to numerically compute the slice of the two-dimensional Fourier transform of a truncated function. This means that Eq. 2.4.1 represents the reflection coefficient of a truncated pressure field $P_R(r)$. The result of this approximation can be better understood by interpreting the truncated field in the following form

$$\tilde{P}_R(r) = P_R(r) \cdot w(r) \qquad (2.4.3)$$

where $w(r)$ = circularly symmetric window.

The circularly symmetric window $w(r)$ is a function of range r and it is of finite range; that is, $r \leq R_{max}$. This causes the pressure field, $\tilde{P}_R(r)$, to be a windowed version of the theoretical pressure field $P_R(r)$.

Let us define:

$\tilde{R}(K)$ = the plane-wave reflection coefficient resulting from processing a windowed version of the pressure field $P_R(r)$.

Then, from Eq. 2.3.12,

$$\tilde{R}(K_x,K_y) = -jK_z\, e^{-jK_z(z+z_0)}\, \frac{1}{2\pi} \iint_{-\infty}^{\infty} \tilde{P}_R(x,y)\, e^{-jK_x x}\, e^{-jK_y y}\, dxdy \tag{2.4.4}$$

Substituting Eq. 2.4.3 in Eq. 2.4.4,

$$\tilde{R}(K_x,K_y) = -jK_z\, e^{-jK_z(z+z_0)}\, \frac{1}{2\pi} \iint_{-\infty}^{\infty} P_R(x,y) \cdot w(x,y)\, e^{-jK_x x}\, e^{-jK_y y}\, dxdy \tag{2.4.5}$$

Convolution $\leftrightarrow$ Fourier Transform Property

If we take the two-dimensional inverse Fourier transform of the two-dimensional convolution of two functions, the result is proportional to the product of their individual two-dimensional

Fourier transforms, that is,

$$Y(K_x,K_y) = H(K_x,K_y) * F(K_x,K_y) = \iint_{-\infty}^{\infty} H(\lambda,\beta)\, F(K_x-\lambda,K_y-\beta)\, d\lambda d\beta \tag{2.4.6}$$

The inverse two-dimensional Fourier transform is

$$y(x,y) = \frac{1}{2\pi} \iint_{-\infty}^{\infty} H(\lambda,\beta) \iint_{-\infty}^{\infty} F(K_x-\lambda,K_y-\beta)\, e^{jK_x x}\, e^{jK_y y}\, dK_x\, dK_y\, d\lambda d\beta \tag{2.4.7}$$

Changing variables,

$$y(x,y) = \frac{1}{2\pi} \iint_{-\infty}^{\infty} H(\lambda,\beta) \iint_{-\infty}^{\infty} F(\hat{\alpha},\hat{\beta})\, e^{j\hat{\alpha}x}\, e^{j\hat{\beta}y}\, d\hat{\alpha}d\hat{\beta}\, e^{j\lambda x}\, e^{j\beta y}\, d\lambda d\beta \tag{2.4.8}$$

$$= 2\pi\, h(x,y) \cdot f(x,y) \tag{2.4.9}$$

Thus,

$$2\pi\, h(x,y) \cdot f(x,y) \overset{\text{2-D FT}}{\longleftrightarrow} H(K_x,K_y) * F(K_x,K_y) \tag{2.4.10}$$

Interpreting Eq. 2.4.5 in the form of Eq. 2.4.10,

$$\tilde{R}(K_x,K_y) = -jK_z\, e^{-jK_z(z+z_0)}\, \frac{1}{2\pi}\, G(K_x,K_y) * W(K_x,K_y) \quad (2.4.11)$$

or

$$\tilde{R}(K_x,K_y) = \frac{1}{2\pi}\, R(K_x,K_y) * W(K_x,K_y) \quad (2.4.12)$$

where $W(K_x,K_y)$ = two-dimensional Fourier transform of $w(x,y)$.

Eq. 2.4.12 indicates that $\tilde{R}(K_x,K_y)$ is proportional to the exact plane-wave reflection coefficient $R(K_x,K_y)$ convolved with the two-dimensional transform of the window. In the process of convolution between the exact Fourier transform of a function with the Fourier transform of the window, we try to choose a window $w(x,y)$ to minimize the effect of wavenumber leakage due to the sidelobes and the degradation in resolution of the wavenumber components due to the main-lobe of the window.

In an attempt to predict the effects of the two-dimensional window on the computation of the plane-wave reflection coefficient, we will present the radial slice of the two-dimensional Fourier transform of a circular pill-box window, a circular Hamming window, and a circular Hanning window. Since the windows are circularly symmetric, their radial slices completely specify the two-

dimensional Fourier transforms. The numerical steps are indicated in Appendix I.

CIRCULAR PILL-BOX WINDOW

The pill-box window is generated by circularly rotating a rectangular window in one dimension. That is,

$$w(r) = w(\sqrt{x^2+y^2}) = 1 \qquad r \leq 1 \qquad (2.4.13)$$

$$= 0 \qquad r > 1$$

In Figure 2.2, we illustrate the radial slice of its two-dimensional Fourier transform. The first zero-crossing, which determines half of the width of the main-lobe, is at approximately

$$K_{w/z} = 4.0$$

and the level of the first side-lobe is about

$$L_S = -17.0 \text{ dB}$$

from the main-lobe.